# Accurate determination of the thickness or mass per unit area of thin foils and single-crystal wafers for x-ray attenuation measurements

C. Q. Tran, C. T. Chantler, Z. Barnea, and M. D. de Jonge
*School of Physics, University of Melbourne, Victoria 3010, Australia*

(Received 1 December 2003; accepted 17 May 2004; published 14 September 2004)

The determination of the local mass per unit area $m/A=\int \rho dt$ and the thickness of a specimen is an important aspect of its characterization and is often required for material quality control in fabrication. We discuss common methods which have been used to determine the local thickness of thin specimens. We then propose an x-ray technique which is capable of determining the local thickness and the x-ray absorption profile of a foil or wafer to high accuracy. This technique provides an accurate integration of the column density which is not affected by the presence of voids and internal defects in the material. The technique is best suited to specimens with thickness substantially greater than the dimensions of the surface and void structure. We also show that the attenuation of an x-ray beam by a nonuniform specimen is significantly different from that calculated by using a simple linear average of the mass per unit area and quantify this effect. For much thinner specimens or in the presence of a very structured surface profile we propose a complementary technique capable of attaining high accuracy by the use of a secondary standard. The technique is demonstrated by absolute measurements of the x-ray mass attenuation coefficient of copper and silver. © *2004 American Institute of Physics.* [DOI: 10.1063/1.1781383]

## I. INTRODUCTION

It is a common problem to require accurate knowledge of the thickness of a foil or of a single-crystal wafer. Sometimes an absolute measurement of the thickness is required, such as in the case of foils or single crystals used to measure the x-ray linear absorption coefficient of a material. At other times it is sufficient to probe the thickness uniformity of a specimen. The accurate determination of thickness becomes particularly difficult in the case of very thin specimens where the variation in the thickness is comparable with the error in the thickness determination.

In this article we shall discuss the measurement of thickness $t$ and a closely related quantity, the mass per unit area ($\rho t$) of thin specimens. We investigate a variety of commonly used methods to measure the local thickness of thin specimens such as weighing a specimen of known area, micrometry, x-ray absorption, and a combination of these techniques. We then propose a "full-foil mapping" method which can determine the local thickness and absorption profile of foils to high accuracy. This method accurately integrates the column density, even in the presence of voids and internal defects. The method is well suited to foils with thicknesses substantially greater than the dimensions of the surface or void structure.

We show that the attenuation of an x-ray beam by a nonuniform specimen is significantly different from a simple linear average of the column density and we quantify this effect. For the case of very thin foils or where the surface profile is very structured, we propose a "transfer" method which, in combination with the "full foil mapping" method, is capable of attaining high accuracy. We apply these techniques to the measurement of the x-ray mass attenuation coefficients of elemental samples.[1–4]

## II. COMMON TECHNIQUES OF THICKNESS DETERMINATION

A well known technique for the accurate determination of the average thickness $t_{av}$ of a foil or wafer of uniform thickness consists of reducing the thickness measurement to the determination of the mass $m$ of a known area $A$ of the specimen. This technique has been widely used in measurements of x-ray attenuation coefficients.[5–8] The mass and area of the specimen can be determined with an accurate balance and an optical traveling microscope. The average thickness $t_{av}$ is obtained from

$$m = \rho V = \rho A t_{av}, \tag{1}$$

where $\rho$ is the density of the specimen material calculated from the atomic weight of the contents of a unit cell divided by the unit cell volume and $V$ is the specimen volume.

A second common technique used to measure thicknesses of thin specimens utilizes high precision micrometers.[9] Figure 1 shows the thickness variation of a typical 100 $\mu$m thick copper foil supplied by GoodFellow. The foil is $\sim$25 mm$\times$25 mm square. The variation in the thickness of the foil was measured using a micrometer with a 5 mm diameter contact region and with 0.5 $\mu$m precision, at 25 points equally spaced over the surface. The accuracy and reproducibility of each measurement was 0.5%, and the variation in local thickness was shown to be 1%–2%.

The thickness of the specimen measured with a micrometer is usually observed to be greater than that measured by weighing of a known area [Eq. (1)]. This is due to the fact that the micrometer tends to measure the maximum thickness of the specimen within the area of its footprint. Also, the use of the density calculated from the unit cell size and the mass of the atoms contained in it results in an average thickness

 

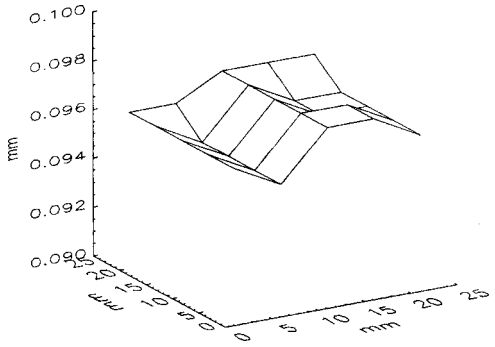


FIG. 1. Micrometer mapping of the variation in thickness of the nominal 100 $\mu$m thick copper foil of Fig. 2.

$t_{av}$, automatically corrected for the presence of voids and cracks, often observed in profilometer scans (Fig. 2).

Even though these methods have been widely used to determine thickness in attenuation measurements, it is obvious from Figs. 1 and 2 that neither the average thickness $t_{av}$ of the entire foil nor the local thickness measured using a micrometer is adequate to determine the precise local mass per unit area of specimens at the location of interest (under the beam footprint in attenuation measurements) due to the thickness variation and the surface and internal structures of the specimens. Errors involved can be up to several percent.

A third technique for calibrating the specimen thickness in attenuation measurements is to measure the x-ray attenuation as a function of the angle $\theta$ between the incident beam and the sample surface.[10–12] The product $(\mu t)$ of the specimen thickness and the linear attenuation coefficient is obtained by fitting the following equation for different values of $\theta$:

$$\ln(I_\theta) = \ln(I_0) - \mu t/\cos\,\theta. \tag{2}$$

However, the main problem with this technique is that the effective thickness of the foil tilted at an angle $\theta$ is only described by $t/\cos\,\theta$ when the variations in thickness and the effect of surface and internal structures are insignificant. This is generally not true in practice. The error involved can be several percent or more. The technique of measuring the transmitted intensity as a function of the angle $\theta$ does however have some merit in determining the particular alignment of the specimen with respect to the x-ray beam.

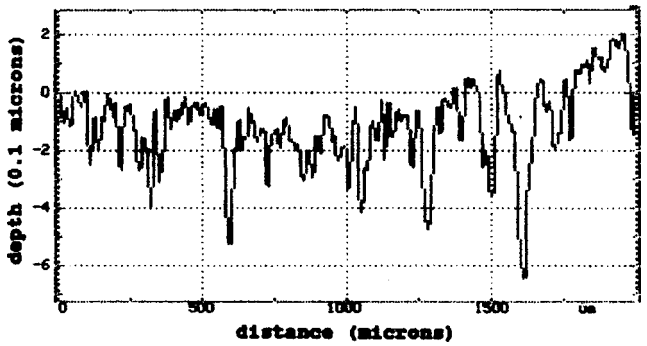


FIG. 2. Profilometer trace showing the microstructure on the surface of a 100 $\mu$m thick copper foil supplied by Goodfellow. Similar surface structures, about 0.5 $\mu$m deep, have been observed in other foils of different thicknesses. The effect of these structures on the determination of foil thickness becomes significant for thinner foils.

The accurate determination of the absorber thickness is one of the crucial unresolved experimental issues causing widespread disagreement in the currently available data of x-ray attenuation coefficients.[13] A good method must take into account both the variation in thickness over the entire specimen as well as the surface and internal structures of the specimen.

## III. DETERMINATION OF THE LOCAL MASS PER UNIT AREA USING PARTIAL X-RAY MAPPING

In our recent measurements of mass attenuation coefficients,[1–4] a combination of methods was employed to determine the foil thickness at the point of incidence of the x-ray beam for a nominally 100 $\mu$m thick Cu foil supplied by Goodfellow. To determine the variation in thickness over the foil area, and to allow for the surface and internal structures of the foils, we combined the results of three very different determinations of the dimensions of the foil by:

(1) obtaining the average thickness $t_{av}$ of the thickest foil by weighing and carefully determining the area of the foil;

(2) mapping the thickness of the foil using a micrometer;

(3) mapping the relative thickness of the central part of the foil using x rays.

The average thickness $t_{av}$ of the entire foil was determined from Eq. (1) where the mass $m$ was obtained by repeated weighing on a microgram scale (resolution 1 $\mu$g), the surface area of the sample A was measured by using an optical comparator (Mitutogo PJ300 with resolution 5 $\mu$m $\times 5$ $\mu$m), and the density $\rho$ used was 8.9331(37) g/cm$^3$.[14] The result obtained was $t_{av} = (0.094\,04 \pm 0.000\,06)$ mm where the uncertainty was obtained by $\%\sigma_{t_{av}} = \sqrt{\%\sigma_p^2 + \%\sigma_m^2 + \%\sigma_A^2}$.

The variation in the thickness of the foil was also measured using a micrometer with a 5-mm-diameter contact region and with 0.5 $\mu$m precision, at 25 points regularly spaced over the surface. The accuracy and reproducibility of each measurement of thickness was 0.5%, and showed that the variation in local thickness was 1%–2%. In fact the average thickness of the specimen obtain by this measurement was $t_{\mathrm{micro},av} = (0.0962 \pm 0.0001)$ mm where the uncertainty is obtained from $\sigma_{t_{\mathrm{micro},av}} = \sqrt{\sigma^2_{t_{\mathrm{micro,loc}}}}/\text{number of grid points}$. The uncertainty of each local measurement $\sigma_{t_{\mathrm{micro,loc}}}$ is 0.0005 mm and the number of grid points is 25. The micrometer measures the maximum thickness over the area of contact, assuming no deformation of the surface by the measurement. Hence this measurement should provide a result greater than the average thickness $t_{av}$ based on density, by an amount corresponding to the surface structure variation.

The variation in $\rho t_{\mathrm{loc}}$ of the specimen was measured by scanning a 20 keV x-ray beam over the central region of the foil following the Beer–Lambert relation:

$$[\mu/\rho]\rho t_{\mathrm{loc}} = \ln(I_0/I), \tag{3}$$

where $[\mu/\rho]$ is the mass attenuation coefficient of the specimen at the beam energy, $I_0$, and $I$ are the incident and the attenuated intensities, respectively, $t_{\mathrm{loc}}$ is the local thickness of that part of the specimen whose area is under the beam footprint. Since $[\mu/\rho]$ is a constant for a given element and

TABLE I. Independent determination of the local thickness of two calibration foils. Results of the thickness determination of the two foils A (275 $\mu$m nominal thickness) and B (275 $\mu$m nominal thickness) are listed in column "$t_{meas}$" with the energies at which the measurements were carried out in column "$E$;" "$\Delta t$ ($\mu$m)" and "%$\Delta t$" show the absolute and relative errors, respectively. Excellent consistency between the measurements of the same foil was achieved as shown in the percent discrepancy between measurements as "% dev."

| Foil | $t_{nom}$ ($\mu$m) | $E$ (keV) | $t_{meas}$ ($\mu$m) | $\Delta t$ ($\mu$m) | %$\Delta t$ | % dev |
|---|---|---|---|---|---|---|
| A | 275 | 22.8 | 276.89 | 0.59 | 0.21 | 0.015 |
| | | 20.0 | 276.80 | 0.84 | 0.30 | −0.015 |
| B | 100 | 24.4 | 102.87 | 0.37 | 0.36 | −0.076 |
| | | 20.0 | 103.02 | 0.32 | 0.31 | 0.063 |
| | | 15.0 | 102.97 | 0.53 | 0.51 | 0.013 |

x-ray photon energy, the variation in the logarithm of the intensity ratio $\ln(I_0/I)$ gives a precise measurement of the variation in the local mass per unit area in the central region of the foil. The outer regions of the foils were held between plastic holders and were therefore not mapped using x rays. An x-ray scan has been used before,[15] but only as a qualitative test of the uniformity of the specimen.

We combine the information from the absolute measurements and the highly precise relative x-ray measurements to obtain the thickness over the actual area through which the beam passed during the attenuation experiment by carrying out the following procedure:

(i) We use a least-square fitting program to match the central $8\times8$ mm$^2$ area whose thickness variation was measured both with the micrometer and the x-ray beam. This allows the footprint center of each micrometer measurement to vary by a typical uncertainty relative to a rigid grid of 0.5 mm, and allows the grid to translate in either direction in 0.5 mm steps. The final match between the two sets of measurements is therefore accurate to better than 0.5 mm with an estimated uncertainty of each point of 0.25 mm in each axis, or 0.1 mm for each grid axis, this is quite adequate given the small variations between thicknesses on adjacent grid points.

(ii) Having found the optimum match of the measurements, we determine the thickness of the actual $1\times1$ mm$^2$ area through which the x-ray beam passed.

(iii) We assume that the local structure (measured by a profilometer) in each region is similar over the entire sample—this has been confirmed in typical locations by direct observation. Then the micrometer thickness map is scaled to yield the overall average thickness and the local region used in the experiment is defined by its location on the x-ray thickness map.

The resulting average thickness of the $1\times1$ mm$^2$ region under the beam footprint in our experiment determined using this combined technique was $0.095\,54\pm0.000\,26$ mm, or a 0.26% accuracy. This compares with $t_{av}=0.094\,04\pm0.000\,06$ mm (or 0.06% accuracy) obtained from the weighing of the known area, and with $t_{micro,av}=0.097\pm0.0005$ mm (or 0.5% accuracy) from the micrometer measurement; the discrepancies are significant at the level of about −1% and +2%, respectively. Note that the percentage error of $t_{av}$ is very small (0.06%) but is about 1% discrepant from the value of the local thickness which the above method has determined to the higher accuracy of 0.26%.

In an experiment with silver, we applied the technique at various energies for two different foils as an independent check of the reliability of the procedure. The results are given in Table I. The local thickness derived from x-ray raster scans at different energies is in excellent agreement. The percent deviation between the results, % dev, is 0.015% for the 275 $\mu$m thick foil and up to 0.076% for the 100 $\mu$m thick foil.

Even though the partial x-ray mapping method has shown excellent reproducibility, its result depends on the effect of the thickness variation of the specimen on the micrometry measurements. An improved technique is therefore required.

## IV. DETERMINATION OF THE LOCAL MASS PER UNIT AREA FOR THICK FOILS: FULL-FOIL MAPPING METHOD

The method of determining the local thickness by partial x-ray mapping described in Sec. III has been replaced in subsequent experiments by a full raster scan and the point-by-point determination of the x-ray absorption over the entire specimen. For simplicity, we assume, in the first instance, that the x-ray beam is of uniform intensity, monochromatic, and collimated to be of square cross section. A raster scan of the specimen in steps roughly equal to the beam dimension results in a map of transmitted x-ray intensities. Knowledge of the intensity of the unattenuated beam leads to a relative absorption map of the specimen governed by the well-known Beer–Lambert relation as discussed previously.

If the x-ray linear attenuation coefficient $\mu$ of the specimen material is accurately known, one can also obtain a map of the absolute local thickness "averaged" over the beam footprint. Without an accurate value of $\mu$, a relative variation of $t_{loc}$ averaged over the beam footprint can still be obtained. These relative values of $t_{loc}$ can be related to $t_{av}$ as discussed in Sec. III.

Figure 3 shows the mapping of the local attenuation $[\mu/\rho]\rho t_{loc}$ of a silver foil roughly 100 $\mu$m thick. The measurement was carried out using a monochromatized 17.0 keV x-ray beam at the Photon Factory synchrotron, beamline 20B. Figures 3(1*l*) and (2*l*) show the measured attenuation of the foil held between the thin jaws of a plastic holder, and of the empty plastic holder, respectively. Figure 3 (3*l*), obtained

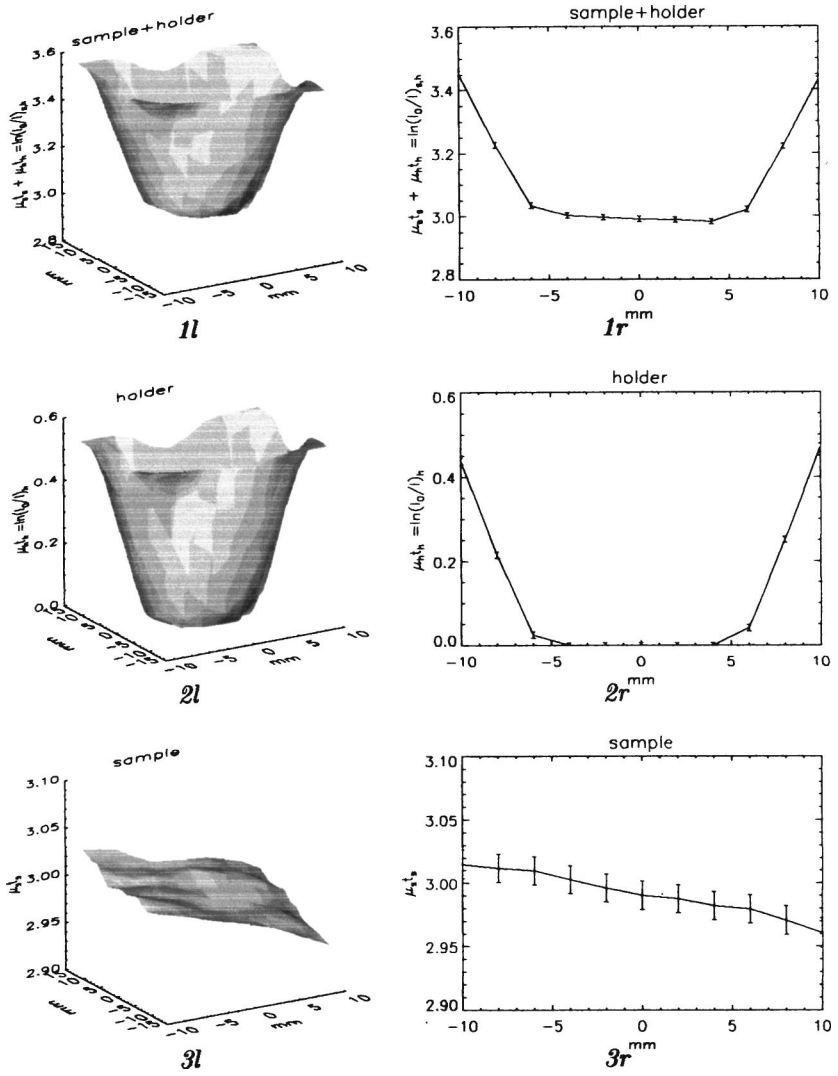


FIG. 3. X-ray mapping to determine the variation in the column density of a 100 $\mu$m thick, 25 mm$\times$25 mm square silver foil supplied by Goodfellow. The images on the left (1*l*, 2*l*, and 3*l*) show the 2D variation in the absorption by the foil mounted in a holder, by a blank holder, and by the foil (by subtracting the first two), respectively. The images on the right (1*l*, 2*l*, and 3*l*) show the corresponding central cross section in one direction with error bars. The final error at the 0.3% level as shown in 3*r* is mainly contributed by statistics and could therefore be improved significantly.

by subtracting Fig. 3(1*l*) from (2*l*), shows an absolute map of $[\mu/\rho]\rho t_{\mathrm{loc}}$, or a relative variation in $\rho t_{\mathrm{loc}}$ of the foil. The attenuation of the plastic holder can also be removed using a fitting procedure as discussed elsewhere.[16] Figure 3(1*r*, 2*r*, and 3*r*) are the center cross section of Fig. 3(1*l*, 2*l*, and 3*l*) along one direction with error-bar indication. The small error of about 0.3% in this determination [Fig. 3(3*r*)] is due mainly to counting statistics and can be significantly improved. Beam nonuniformity will give rise to inaccuracies due to the convolution of the beam intensity profile with the unknown thickness variation and structures over the beam footprint. Nonmonochromaticity of the x-ray beam due to harmonic contributions needs to be avoided or allowed for as-discussed elsewhere.[17]

The absolute value of the local mass per unit area averaged over the footprint of the x-ray beam can be determined by making use of the average thickness $t_{av}$, obtained from the weight per unit area, and relating this to the attenuation variation as determined from the x-ray raster scan. Combining Eqs. (1) and (2), we find

$$[\mu/\rho] = \frac{\sum_{i=1}^{N} [\ln(I_0/I)_i/N]}{m/A}, \tag{4}$$

where the averaging is over the $i$ steps of the raster scan. Hence the local mass per unit area $(\rho t_j)$ is given by

$$(\rho t_{\mathrm{loc},j}) = \ln(I_0/I)_j \frac{m/A}{\sum_{i=1}^{N} [\ln(I_0/I)_i]}, \tag{5}$$

where $(\rho t_{\mathrm{loc},j})$ has been corrected by allowing for the thickness variation over the entire foil.

Provided the beam intensity and the foil over the beam footprint are uniform, the error in $(\rho t_{\mathrm{loc},j})$ derived from Eq. (4) is quite small and due entirely to the uncertainties in $m$, $A$, and counting statistics.

The uncertainty due to the nonuniformity of the specimen and of the beam intensity can be estimated by rotating the foil about the x-ray beam. Variations in the intensity recorded for different positions during the rotation will be due both to the nonuniform beam intensity and to the nonuniform

($\rho t$) over the small area of the beam footprint. Separation of the beam and specimen nonuniformity requires the additional use of a slit whose size will determine the resolution of the measurement.

## V. EFFECT OF THICKNESS VARIATION OVER THE BEAM FOOTPRINT

The Beer–Lambert relation is defined for a narrow, parallel, and monochromatic beam attenuated by a foil whose thickness over the beam footprint is perfectly uniform. In general, the thickness $t$ under the footprint will vary. This value of $t$ is different from the linear average of the foil thickness over the footprint due to the logarithmic nature of the relationship between the thickness and the attenuation. This has been demonstrated using particular geometrical assumptions such as linear-wedge-shaped, sinusoidally shaped and square-wave-shaped foils.[18]

In this section we will consider a more practical case when the thickness variation over the footprint of the beam can be represented by a normal distribution:

$$f(t) = \frac{1}{\sqrt{2\pi}\sigma} e^{-(t-\bar{t})^2/2\sigma^2}, \tag{6}$$

where $\bar{t}$ and $\sigma$ are the mean and the standard deviation of the thickness distribution. Assuming that the beam intensity is uniform, the attenuated intensity is then:

$$I = \int_{-\infty}^{\infty} I_0 f(t) e^{-[\mu/\rho]\rho t} dt$$

$$= I_0 \frac{1}{\sqrt{2\pi}\sigma} \int_{-\infty}^{\infty} e^{-(t-\bar{t})^2/2\sigma^2} e^{-[\mu/\rho]\rho t} dt, \tag{7}$$

where for thick targets ($\sigma \ll \bar{t}$) the integration can be from $-\infty$ to $+\infty$. Using

$$\int_{-\infty}^{\infty} e^{-p^2t^2 \pm qt} dt = \frac{\sqrt{\pi}}{|p|} e^{q^2/4p^2}, \tag{8}$$

Eq. (7) becomes

$$I = I_0 e^{-[\mu/\rho]\rho(\bar{t} - [\mu/\rho]\rho\sigma^2/2)}. \tag{9}$$

Equation (9) indicates that the apparent thickness ($\bar{t} - [\mu/\rho]\rho\sigma^2/2$) obtained by using attenuation measurements with a known $[\mu/\rho]$ is smaller than the linearly averaged thickness within the beam footprint by an amount of $[\mu/\rho]\rho\sigma^2/2$. Conversely, if the column thickness $\bar{t}$ within the beam footprint can be determined by linear averaging, for example by using the techniques discussed in Secs. III and IV, then the $[\mu/\rho]_{\text{meas}}$ obtained in measurements of attenuation coefficients will be overestimated by a factor of ($[\mu/\rho]\rho\sigma^2/2\bar{t}$). In fact, this effect is true for arbitrary variation in thickness of the specimen where $\sigma$ is the root-mean-square of the thickness variation. This suggests, interestingly, that the linearly averaged column density should not be used in the Beer–Lambert relation to determine mass attenuation coefficients in the cases of thin foils with structures of size comparable to their thickness. This effect is significant and must be corrected for in attenuation measurements, particularly of heavy elements in the low-energy range.

For example, for gold ($\rho = 18.85\ \text{g/cm}^3$), at 5 and 10 keV the typical thicknesses [for which $\ln(I_0/I) \approx 2$] are 2 and 10 $\mu$m, respectively. The mass attenuation coefficients of these foils are $\sim 638$ and 110 $\text{cm}^2/\text{g}$. Assuming that the surface structures are of the order of 1 $\mu$m for both foils, the errors are $638 \times 18.85 \times 10^{-8}/(2 \times 2 \times 10^{-4}) \approx 30\%$ and $110 \times 18.85 \times 10^{-8}/(2 \times 10^{-3}) \approx 1\%$. It is thus obvious that for gold below 10 keV single-foil measurements are inadequate.

To minimize this error, one must use not only good quality foils (small $\sigma$) but also the thickest possible foils (largest $\bar{t}$) at the highest practicable energy (smallest $\mu$).

## VI. THIN AND HIGHLY STRUCTURED SPECIMENS: TRANSFER METHOD

As we have already indicated, the accurate determination of the local mass per unit area becomes particularly difficult in the case of thin specimens for which the variation becomes comparable with the error in the determination of ($\rho t$) and where the effect of surface cracks and voids makes a sizable contribution to the effective value of ($\rho t$). In such cases there are considerable advantages in a comparison of the mass per unit area of the thin specimen with that of a thicker specimen characterised by the full-foil x-ray mapping method we have already described in Sec. IV. To determine the mass per unit area of the thicker specimen one chooses an x-ray energy for which the value of $[\mu/\rho]\rho\sigma^2/2$ is small compared to $t$. For the comparison measurement one chooses an x-ray energy for which the absorption by the thinner specimen is easily measured and that of the thicker specimen is not too great. At this energy the absorption by the two specimens is measured in turn.

By comparing the attenuation levels measured for foils of different thickness under the same experimental conditions, the effective mass per unit area of the thinner foil can be related to that of the thicker, calibrated foil:

$$\rho t_{\text{thin,eff}} = \frac{\ln(I_0/I)_{\text{thin}}}{[\mu/\rho]} = \rho t_{\text{cal}} \frac{\ln(I_0/I)_{\text{thin}}}{\ln(I_0/I)_{\text{cal}}}, \tag{10}$$

where subscripts thin and cal indicate quantities related to the thinner and the thicker, calibrated foil, respectively. This mass per unit area ($\rho t_{\text{thin,eff}}$) should not be considered a precise value of the linear average of the mass per unit area of the thinner foil under the beam footprint. However, the mass attenuation coefficients $[\mu/\rho]$ derived from this effective mass per unit area are not affected by the error due to the surface structure of the thinner foil:

$$[\mu/\rho]_{\text{meas}} = \frac{\ln(I_0/I)_{\text{thin}}}{\rho t_{\text{thin,eff}}} = \frac{\ln(I_0/I)_{\text{thick}}}{\rho t_{\text{thick}}} \approx [\mu/\rho], \tag{11}$$

where the first equality reflects the procedure of the derivation of $[\mu/\rho]$ from the attenuation measurement, the second is a result of the transfer procedure, and the approximate equality on the right-hand side involves a small and generally insignificant error from the effect of the nonuniformity of the thick specimen as discussed in Sec. V. This shows that even though the local mass per unit area of the thin foil determined from this transfer scheme is different from the linear average of ($\rho t$), the value of the mass attenuation co-

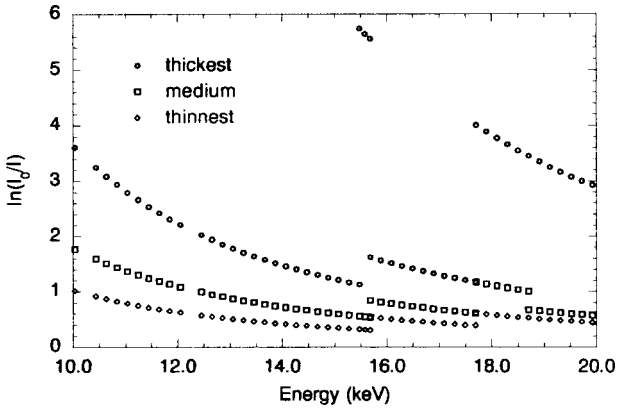


FIG. 4. Multiple-foil measurements of attenuation over an extended energy range illustrating the thickness transfer procedure.

efficients calculated from the measured intensity ratios does accurately follow the ideal Beer–Lambert relation.

The advantages of this transfer procedure in which the thickness of the thin specimen is referred to that of the thicker specimen are:

(i) the results of the measurements are not affected by a nonuniform intensity distribution of the x-ray beam;
(ii) a specific area of the size of the x-ray beam footprint on the thin foil can be selected and used in the thickness comparison with the thicker foil: effects due to the thickness variation of the thinner foil are thus avoided;
(iii) the thinner foil can be used in measurements at lower x-ray energies for which the thicker specimen becomes too absorptive; this feature is particularly useful in extending the energy range of measurements of the x-ray mass attenuation coefficients.

An example of this procedure is demonstrated in Fig. 4. In the energy range between 17.6 and 20 keV the thickest foil (100 $\mu$m Cu) is used as the calibration foil whose local thickness was accurately determined by the procedure discussed in Sec. IV. The thicknesses of the other foils in the same energy range were determined by comparing their attenuations to that of the calibration foil. The thickest foil in this energy range was then replaced by a new foil which is the thinnest foil in the next energy region (15.6–17.6 keV). The thickness of this new foil was determined by comparing its attenuation to those of the two remaining foils. This procedure was then repeated at lower energies and enabled us to bring the entire set of measurements onto a single scale whose accuracy is of the same order as the accuracy with which we are able to determine the thickness of the thickest foil.

## VII. DISCUSSION

We note that the thickness determined by this method which calibrates both the micrometer map and the x-ray map to the reference value of $t_{av}$ obtained from the mass of a known area, is a direct measurement of the amount of material seen by the incident beam. As a consequence, the derived mass attenuation coefficient is independent of the value used for $\rho$, the density of the specimen. Linear attenuation coefficients from measurements using other methods of thickness determination are dependent on the density of the particular specimens used and should therefore not be compared[9] without allowance for density differences.[19–21]

Uncertainties in the technique presented in Secs. IV and VII are due to uncertainties in the determination of the mass $m$, area $A$, and statistics. For a regularly shaped specimen with straight edges such errors can be quite small.

The techniques presented in this article are only applicable to high purity specimens. The effect of impurities may be significant, especially when the impurities are of higher atomic number than the specimen material. The correction to the mass attenuation due to contamination by these elements with atomic numbers $Z_i$ at corresponding concentration levels $C_i$% can be calculated from:

$$\%_{\text{correction}} = \frac{[\mu/\rho]_{Z_0} \times Z_0\% + \Sigma[\mu/\rho]_{Z_i} \times C_i\%}{[\mu/\rho]_{Z_0}}, \qquad (12)$$

where $Z_0$ is the atomic number of the specimen material.

In the case of thin single-crystal wafers the orientation and x-ray energy may accidentally combine to satisfy the Laue–Bragg diffraction conditions.[3,4] Fortunately the sharp inconsistency of the attenuation and the great sensitivity of the measurement to wafer orientation allow one to recognize and avoid this condition.

The most accurate technique to determine the thickness of a thin foil involves an x-ray raster scan of the entire foil to map the variation in $(\rho t)$ of the specimen as a function of position. This map is then scaled to the average thickness of the entire foil obtained by measurement of the mass of its known area. For much thinner specimens, where the surface and the internal structures within the beam footprint is significant, the thickness transfer procedure should be considered.

## ACKNOWLEDGMENTS

The authors acknowledge the support of both the Australian Research Council and the Australian Synchrotron Research Program, which is funded by the Commonwealth of Australia under the Major National Research Facilities Program.

[1] C. T. Chantler, C. Q. Tran, D. Paterson, D. Cookson, and Z. Barnea, Phys. Lett. A **286**, 338 (2001).
[2] C. T. Chantler, C. Q. Tran, D. Paterson, D. Cookson, and Z. Barnea, Phys. Rev. A **64**, 062506 (2001).
[3] C. Q. Tran, C. T. Chantler, and Z. Barnea, Phys. Rev. Lett. **90**, 257401 (2003).
[4] C. Q. Tran, C. T. Chantler, Z. Barnea, D. Paterson, and D. J. Cookson, Phys. Rev. A **67**, 042716 (2003).
[5] L. Gerward, Acta Crystallogr., Sect. A: Found. Crystallogr. **39**, 322 (1983).
[6] L. Gerward, Acta Crystallogr., Sect. A: Found. Crystallogr. **45**, 1 (1989).
[7] W. Dachun, D. Xunliang, W. Xinfu, Y. Hua, Z. Hongyu, S. Zinyin, and Z. Guanghua, Nucl. Instrum. Methods Phys. Res. B **71**, 241 (1992).
[8] W. Dachun, Y. Hua, and W. Xin-Min, Nucl. Instrum. Methods Phys. Res. B **86**, 236 (1994).
[9] L. Gerward, J. Phys. B **14**, 3389 (1981).
[10] L. D. Calvert, R. C. G. Killean, and A. McL. Mathieson, Acta Crystallogr., Sect. A: Found. Crystallogr. **31**, 855 (1975).
[11] J. L. Lawrence and A. McL. Mathieson, Acta Crystallogr., Sect. A: Found.

Crystallogr. **32**, 1002 (1976).
[12] J. L. Lawrence, Acta Crystallogr., Sect. A: Found. Crystallogr. **33**, 343 (1977); **35**, 845 (1979).
[13] C. T. Chantler, Z. Barnea, C. Q. Tran, J. Tiller, and D. Paterson, Opt. Quantum Electron. **31**, 495 (1999).
[14] D. R. Lide, *Handbook of Chemistry and Physics*, 76th ed. (CRC, London, 1996), pp. 4–139.
[15] B. R. Kerur, S. R. Thontadarya, and B. Hanumaiah, Appl. Radiat. Isot. **42**, 571 (1991).
[16] M. D. de Jonge, Z. Barnea, C. Q. Tran, and C. T. Chantler, Meas. Sci. Technol. **15**, 1811 (2004).
[17] C. Q. Tran, Z. Barnea, M. de Jonge, B. B. Dhal, D. Paterson, D. Cookson, and C. T. Chantler, X-Ray Spectrom. **32**, 69 (2003).
[18] T. A. Boster, J. Appl. Phys. **44**, 3776 (1973).
[19] J. F. Mika, L. J. Martin, and Z. Barnea, J. Phys. C **18**, 5215 (1985).
[20] D. C. Creagh and J. Hubbell, Acta Crystallogr., Sect. A: Found. Crystallogr. **43**, 102 (1987).
[21] D. C. Creagh and J. Hubbell, Acta Crystallogr., Sect. A: Found. Crystallogr. **46**, 402 (1990).